ARTICLE

Cell Research (2004); 14(3): 188-196
http://www.cell-research.com

Induction of antiproliferative effect by diosgenin through activation of p53, release of apoptosis-inducing factor (AIF) and modulation of caspase-3 activity in different human cancer cells

Cecile CORBIERE[1], Bertrand LIAGRE[1,*], Faraj TERRO[2], Jean-Louis BENEYTOUT[1]

[1]*Laboratoire de Biochimie, UPRES EA 1085, Faculté de Pharmacie, 2 rue du Docteur Marcland, 87025 Limoges Cedex, France.*
[2]*Service d'Histologie et Biologie Cellulaire, Faculté de Médecine, 2 rue du Docteur Marcland, 87025 Limoges Cedex, France.*

ABSTRACT

Previously, we demonstrated that a plant steroid, diosgenin, altered cell cycle distribution and induced apoptosis in the human osteosarcoma 1547 cell line. The objective of this study was to investigate if the antiproliferative effect of diosgenin was similar for different human cancer cell lines such as laryngocarcinoma HEp-2 and melanoma M4Beu cells. Moreover, this work essentially focused on the mitochondrial pathway. We found that diosgenin had an important and similar antiproliferative effect on different types of cancer cells. In addition, our new results show that diosgenin-induced apoptosis is caspase-3 dependent with a fall of mitochondrial membrane potential, nuclear localization of AIF and poly (ADP-ribose) polymerase cleavage. Diosgenin treatment also induces p53 activation and cell cycle arrest in the different cell lines studied.

***Keywords*:** diosgenin, apoptosis, p53, AIF, caspase, cancer cells.

INTRODUCTION

Programmed cell death or apoptosis plays an important role in normal development and is impaired in many types of cancer. The tumor suppressor protein p53 is a principal factor in regulation of growth arrest as well as apoptosis [1]. Many apoptotic signals are mediated to the cell death machinery via p53[2]. It interacts with other proteins or functions as a transcription factor[3, 4]. Indeed, in response to various types of stress, p53 becomes activated and, as a consequence, cells can undergo marked phenotype changes, ranging from increased DNA repair to senescence and apoptosis[5].

Apoptosis is characterized by chromatin condensation and DNA fragmentation, and is mediated by the cysteine protease family called caspases[6]. Mitochondria are involved in a variety of key events, including release of caspase activators, changes in electron transport, loss of mitochondrial membrane potential ($\Delta\psi m$), and participation of both pro- and anti-apoptotic Bcl-2 family proteins [7-9]. Alterations in mitochondrial structure and function have been shown to play a crucial role in caspase-9-dependent apoptosis[10] by releasing apoptotic factors from mitochondria including cytochrome c[11]. In this manner, released cytochrome c interacts with Apaf-1 and pro-caspase-9 to form the apoptosome. Then caspase-9 cleaves and activates caspase-3, the executioner caspase, which cleaves poly (ADP-ribose) polymerase (PARP) and activates endonucleases leading to DNA fragmentation [10].

In response to apoptogenic stimuli, the mitochondrial protein apoptosis-inducing factor (AIF) translocates through the outer mitochondrial membrane to the cytosol and to the nucleus, resulting in the induction of nuclear chromatin condensation and large DNA fragmentation in a caspase-independent manner[12-15].

Previously, we showed that diosgenin, a plant steroid, altered cell cycle and induced apoptosis in the human osteosarcoma 1547 cell line[16]. Recently, we compared diosgenin with two other plant steroids (hecogenin and tigogenin) in the same cell line and among these three plant steroids, diosgenin appeared to be the most effective in inducing cell death[17]. In order to know if results obtained with diosgenin on 1547 cells could be extended to other types of cancer cells, we tested this molecule on laryngocarcinoma HEp-2 cells and melanoma M4Beu cells. Moreover, to gain further insight into the mechanisms by which diosgenin induces apoptosis in human cancer cells, we examined in this study the functional status of caspases on apoptosis rate and the effect of diosgenin on mitochondrial integrity in the two human cancer cell lines (HEp-2 and M4Beu cells).

[*]Correspondence: Bertrand LIAGRE, Tel: +33-555-43-58-39; Fax: +33-555-43-58-39; E-mail: bertrand.liagre@unilim.fr

MATERIALS AND METHODS

Cell lines, cell culture and treatment

The HEp-2 human laryngocarcinoma and M4Beu human melanoma cell lines were kindly provided respectively by Professor M. Cogné (Laboratoire d'Immunologie, Faculté de Médecine de Limoges, France), and Professor C. Delage (Laboratoire de Chimie Physique et Minérale, Faculté de Pharmacie de Limoges, France). HEp-2 cells were seeded at 3.5×10^3 cells/cm^2 and grown in Dulbecco's modified Eagle medium (Gibco BRL, Cergy-Pontoise, France) containing 10% fetal calf serum (FCS), 100 U/ml penicillin and 100 µg/ml streptomycin. M4Beu cells were seeded at 5×10^3 cells/cm^2 and grown in Eagle's minimum essential medium supplemented with 10% FCS, 1% vitamins, 1% non essentials aminoacids, 20 µg/ml gentamicin. Cultures were maintained in a humidified atmosphere with 5% CO_2 at 37°C. Cell viability was determined by the trypan blue dye exclusion method. For all experiments and for all cell lines, cells were allowed to adhere and grow for 3 d in culture medium prior to exposure to diosgenin. A stock solution of 10^{-2} M diosgenin was prepared in ethanol and diluted in culture medium to give a final concentration of 20-100 µM. The same amount of ethanol was added to control cells. We worked with 20-100 µM of diosgenin to compare results obtained with 1547 cells[16].

Cell proliferation assay

Measurement of cell proliferation was determined using the 3-(4, 5-dimethylthiazol-2-yl)-2,5-diphenyltetrazolium bromide (MTT) assay. Cells were plated in 96-well culture plates and grown 3 d before treatment with 20-100 µM diosgenin for 24-96 h. MTT was carried out daily as previously described[18] and experiments were performed in sextuple assay.

Protein expression analysis

Cells were cultured in 150 cm^2 tissue culture flasks. After 40 µM diosgenin treatment, adherent cells were trypsinized and pooled with the floating cell fraction. Western blot analysis was performed as previously described[16] using the primary monoclonal antibodies β-actin [mouse anti-human β-actin (1:5000), Sigma], Bcl-2 [mouse anti-human Bcl-2 (1:1000), Dako], Bax [mouse anti-human Bax (1: 2000), Immunotech], p53 [mouse anti-human p53 (1:1000), Santa Cruz Biotechnology], PARP [mouse anti-human PARP (1:100), Santa Cruz Biotechnology] and respective secondary polyclonal antibodies conjugated with peroxidase (Dako). Blots were visualized using enhanced chemiluminescence reagents (Amersham Biosciences) and immediately exposed to X-ray films.

For subsequent immunofluorescent labelling of phospho-p53 protein and PARP p85 fragment, adherent cells were fixed in glutaraldehyde-formaldehyde (0.25%-1%) in Tris buffered saline (TBS, pH 8) for 2 min at 37°C and washed twice with TBS. Cells were permeabilized with 0.1% sodium citrate-0.1% triton X100 for 20 min at room temperature, and non-specific Fc-binding sites were blocked by incubation with 0.1% (w/v) bovine serum albumin (BSA) in TBS pH 8 for 45 min. Cells were incubated overnight at 4°C with mouse monoclonal antibody anti-human phospho-p53 [1:200 in TBS/ 0.1% (w/v) BSA; Calbiochem] or mouse polyclonal antibody anti-human PARP p85 fragment [1/500 in TBS/0.1% (w/v) BSA; Promega]. After washing 3×5 min with TBS, cells were labelled for 40 min with biotinylated anti-mouse IgG (1:200 in TBS; Interchim). Cells were washed and labelled for 40 min with FITC-conjugated streptavidin (1:1000 in TBS; Dako), washed again three times with TBS, and mounted with immumount (Shandon). Immunofluorescence pictures were taken with a Nikon microscope ECLIPSE E800 (Nikon Corporation).

Cell cycle analysis

Cells were seeded in 25 cm^2 tissue culture flasks and cultured in 10% FCS medium without or with diosgenin (40 µM) for 12 and 24 h. Floating and adherent cells were combined and cell viability was determined by the trypan blue dye exclusion method. For DNA content analysis, 10^6 cells were fixed and permeabilized in 70% ethanol, washed in phosphate-buffered saline (PBS, pH 7.4) treated with RNase (40 U/µl, Boehringer Mannheim) and stained with propidium iodide (PI) (50 µg/ml). Flow cytometric analyses were performed as previously described[16].

Apoptosis quantification : DNA fragmentation

Cells were cultured in 6-well culture plates. After diosgenin treatment, apoptosis was quantified on pooled cells (floating and adherent) using the 'cell death' enzyme-linked immunosorbent assay (ELISA) (Cell Death Detection ELISA^{plus}, Roche Diagnostics). Cytosol extracts were obtained according to the manufacturer's protocol and apoptosis was measured as previously described[16].

Mitochondrial membrane potential (Δψm)

Δψm was estimated using 5,5',6,6'-tetrachloro-1,1',3,3'-tetraethylbenzimidazole carbocyanide iodide (JC-1, Molecular Probes). JC-1 is a fluorescent compound that exists as a monomer at low concentrations. At higher concentrations, JC-1 forms aggregates. Fluorescence of the monomer is green, whereas that of the JC-1 aggregate is red. Mitochondria with intact membrane potential concentrate JC-1 into aggregates which fluoresce red, whereas de-energized mitochondria cannot concentrate JC-1 and fluoresce green [19].

Cells were grown for 72 h before treatment with 40 µM diosgenin for 6 and 24 h. Control cells were grown in medium containing the same amount of ethanol as treated cells. Adherent cells were incubated in 1 ml of medium containing JC-1 (1 µg/ml) for 30 min at 37°C and pictures were taken with a Nikon microscope ECLIPSE E800.

Cytosol/Mitochondria/Nuclear fractionation for AIF localization

Fractionation was realised using Mitochondria/Cytosol Fractionation Kit (BioVision). Floating and adherent cells were combined and resuspended in 0.5 ml of cold cytosol extraction buffer. After 10 min on ice, cells were homogenized in a Potter homogenizer and centrifuged for 10 min at 700 g to separate unlysed cells and nuclei from first supernatant (S1). The pellet of unlysed cells and nuclei was resuspended in nuclear buffer [500 mM KCl, 25 mM HEPES (pH 7.8), 1 mM PMSF, 100 µM DTT, 10% glycerol] centrifuged 10 min at 20,000 g and the supernatant (S2) was collected as the nuclear fraction. Then, S1 supernatant was centrifuged at 10,000 g for 30 min. The new supernatant (S3) represented the cytosolic fraction, whereas the pellet, resuspended in mitochondria extraction buffer, represented the mitochondrial fraction. The protein concentration in cytosolic and nuclear fractions were determined by the Bradford method. Equal amounts of cytosolic and nuclear fractions from control and treated

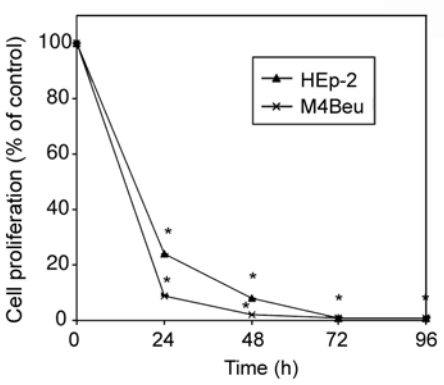

Fig 1. Inhibition of proliferation in HEp-2 and M4Beu cells after diosgenin treatment. After 3 d, cells were cultured in 10% FCS medium and treated with 40 µM diosgenin for 24-96 h. Results are presented as percentage of control (untreated cells) and values are expressed as means ± SD of six experiments (*p-value relative to control group, $p<0.05$).

cells were subjected to Western blot analysis of AIF using rabbit anti-human AIF (1:1000, Sigma) and β-actin (mouse anti-human β-actin (1:5000), Sigma) antibodies.

Caspase activities

After 40 µM diosgenin treatment for 12 and 24 h, cells were homogenized in lysis buffer according to the manufacturer's protocol (CaspACE™Assay System Fluorometric, Promega). Fluorometric assays were conducted in white opaque tissue culture plates (Falcon, Becton Dickinson Labware, NJ, USA) and all measurements were carried out in triplicate. First, 100 µl of assay buffer (10 mM DTT, DMSO, Caspase Buffer) (Promega) were added to each well. Peptide substrates for caspase-3 [Ac-DEVD-7-amino-4-methylcoumarin (AMC)] and caspase-9 (Ac-LEHD-AMC) were added to each well to a final concentration of 2.5 mM. Caspase inhibitor (Ac-DEVD-CHO) was also used at a concentration of 2.5 mM just before the addition of the substrate. The supernatant of each cell lysate collected was added to each well to start the reaction. Background fluorescence was determined in wells containing assay buffer and substrate without cell lysate. Assay plates were incubated at 37 °C for 1 h for the measurement of both caspase activities. Fluorescence was measured with a microplate reader (Fluorolite 1000, Dynatech Laboratories, Dynex Technologies, Labsystems) using 360 nm excitation and 460 nm emission filters. Raw data [Relative Units of Fluorescence (RUF)] corresponded to the concentrations of AMC released[20].

Statistical analysis

The median and standard deviation (SD) were calculated using Excel (Microsoft Office, Version 98). Statistical analysis of differences was carried out by analysis of variance (ANOVA) using StatView (Version 5.0). $p<0.05$ (Fisher's PLSD test) was considered to indicate significance.

RESULTS

Diosgenin and cell proliferation

Cells were cultured in 10% FCS-medium with or without 20-100 µM diosgenin for 24-96 h and cell proliferation was evaluated by the MTT test. Under our experimental conditions, 40 µM diosgenin caused a significant decrease in proliferation as early as 24 h after treatment on HEp-2 and M4Beu cells [76% ($p<0.05$) and 91% ($p<0.05$) respectively] and continued to decline until 96 h (Fig 1). As the concentration of 20 µM weakly inhibit cell proliferation [10 % for both cell lines, $p<0.05$ (data not shown)], we choose 40 µM for following experiments.

p53 expression and cell cycle analysis

To ascertain the potential mechanisms by which diosgenin inhibited cancer cell proliferation rate, we studied the expression of p53 and the distribution of the cell cycle (Fig 2 and 3 respectively) in HEp-2 and M4Beu cells. Western blot analysis of p53 showed no significant difference in expression for HEp-2 treated cells versus control (Fig 2A) and a decrease for M4Beu treated cells (2-fold versus control, $p<0.05$) (Fig 2C). However, immunohistochemistry analysis revealed that activated-p53 (phosphorylated-p53) was expressed and localized in a diffuse manner in treated cells (Fig 2B, b and 2D, d for HEp-2 and M4Beu cells respectively) compared to controls (Fig 2B, a and Fig 2D, c) as previously described in 1547 cells[17].

Moreover, cell cycle analysis showed cell cycle arrest for HEp-2 and M4Beu cells, as for 1547 cells [16]. Indeed, diosgenin blocked HEp-2 cells in the S phase at 24 h and M4Beu cells in the G_2/M phase at 12 h (Fig 3).

DNA fragmentation and analysis of Bax/Bcl-2 ratio

Quantitative determination of cytoplasmic histone-associated-DNA-fragments (mono- and oligonucleosomes) was performed with ELISA in HEp-2 and M4Beu cells. Results showed that DNA fragmentation was enhanced (2.5-fold, $p<0.05$) in treated HEp-2 cells and strongly induced in treated M4Beu cells (23-fold, $p<0.05$) compared to each control (Fig 4).

Apoptotic ratio (Bax/Bcl-2) obtained with Western blot indicated that only the ratio for M4Beu cells increased (1.6-fold versus control, $p<0.05$) in contrast to HEp-2 cells after diosgenin treatment (Fig 5B and A, respectively).

Effect of diosgenin on mitochondrial membrane potential (Δψm)

Δψm was analysed in adherent cell lines after 6 and 24 h treatment with diosgenin using JC-1, a lipophilic cationic probe. Fluorescence observed in Fig 6 showed Δψm

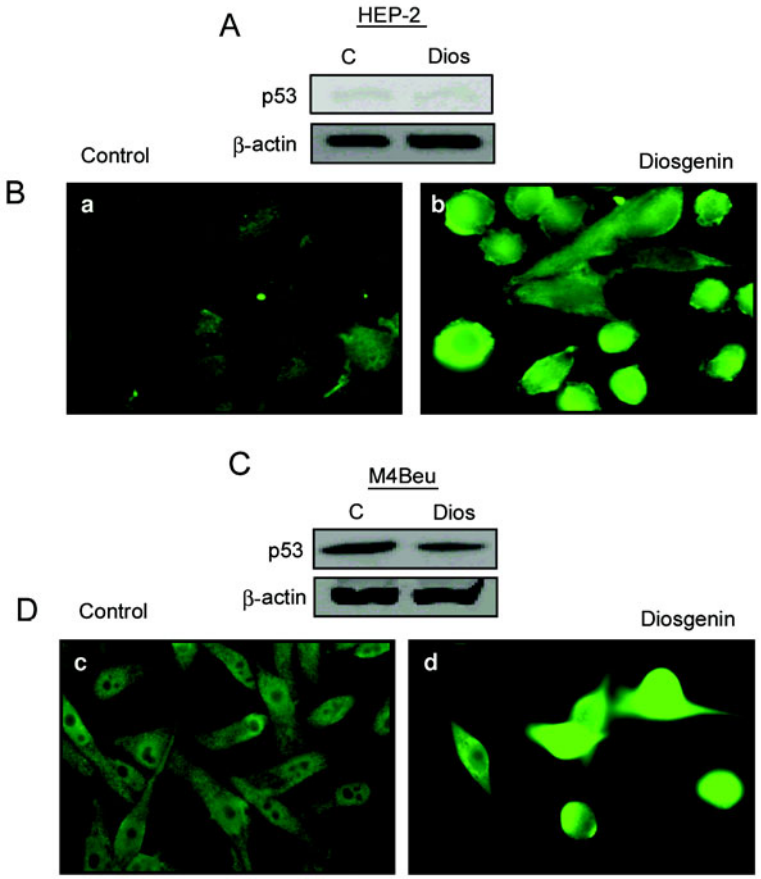

Fig 2. (**A** and **C**), p53 Western blot analysis in HEp-2 and M4Beu cells. Total protein was extracted from the cells and separated on 10% SDS-PAGE gel. Cellular expressions of p53 and β-actin were estimated using mouse anti-human p53 and β-actin antibodies respectively. Quantification of each band was performed by densitometry analysis software and results were expressed relative to control. One of three representative experiments is shown. (**B** and **D**), Immunofluorescence detection of phospho-p53 protein in HEp-2 and M4Beu cells. Cells were treated or not (photos a and c) with 40 μM diosgenin for 24 h (photos b and d). Immunofluorescence pictures were taken with a Nikon microscope ECLIPSE E800(×500).

differences. At 6 h, treated HEp-2 cells showed an increase of green fluorescence compared to control, indicating that $\Delta\psi m$ was diminished (Fig 6). This result was confirmed by the 24 h treatment with diosgenin (data not shown). In return, we showed that diosgenin was less effective on M4Beu cells (Fig 6).

Subcellular redistribution of apoptosis inducing factor (AIF)

Involvement of AIF in diosgenin-induced apoptosis was analysed by Western blot on subcellular fractions of adherent and floating cells. The quality of cytosolic and nuclear fractions is shown by β-actin expression (Fig 7). After 40 μM diosgenin for 6 h, we observed a nuclear accumulation of AIF in HEp-2 and M4Beu cells (Fig 7).

Caspase activities

Caspase-3 and -9 activities were analysed in each cell lines. Caspase-3 and -9 activities were unchanged at 12 h in HEp-2 cells (Fig 8). At 24 h, their activities were enhanced significantly (1.2-fold for caspase-9 and 1.6-fold for caspase-3 versus controls, $p<0.01$) (Fig 8).

In M4Beu cells, caspase-9 activity was moderately induced at 12 and 24 h [1.3-($p<0.01$) and 1.2-fold ($p<0.05$) at 12 and 24 h respectively versus controls] (Fig 8), whereas caspase-3 activity was more markedly induced at the same time (3.4- and 2.2-fold respectively versus controls, $p<0.01$) (Fig 8).

PARP cleavage

Since PARP is a substrate for activated caspases and is typically cleaved and inactivated during the apoptotic process, we analysed PARP cleavage on adherent and floating cells after 24 h treatment with diosgenin. Partial

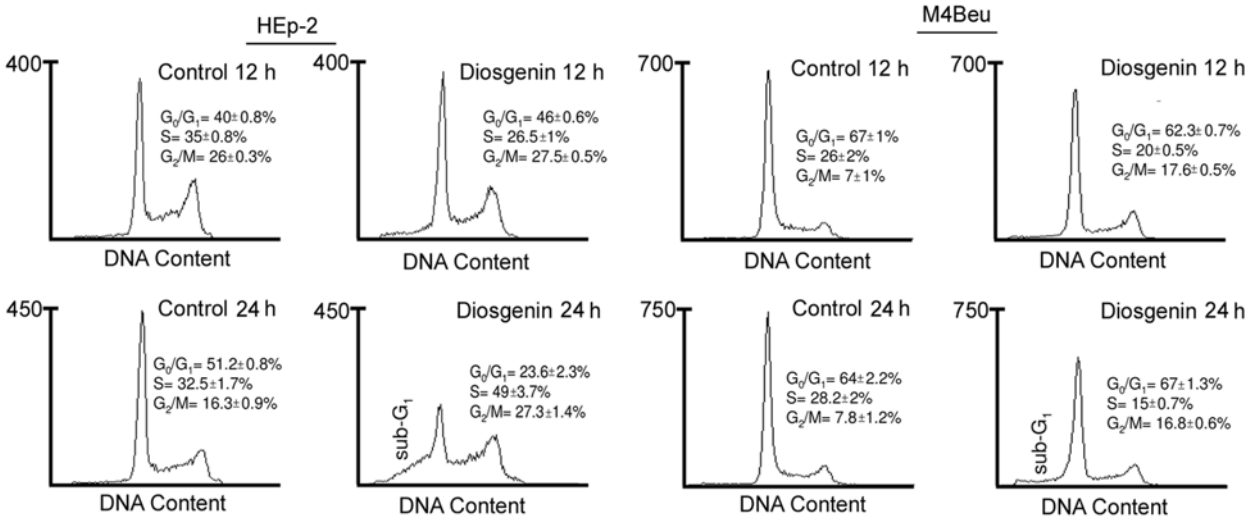

Fig 3. Cell cycle analysis of HEp-2 and M4Beu cells. Cells were treated or not with 40 μM diosgenin for 12 and 24 h. Cell phase distribution was determined by PI staining and Facs analysis. The experiments were performed three times, representative results are shown. Diosgenin treated cells showed a cell cycle arrest in S phase at 24 h for HEp-2 and in G_2/M phase after 12 h for M4Beu cells.

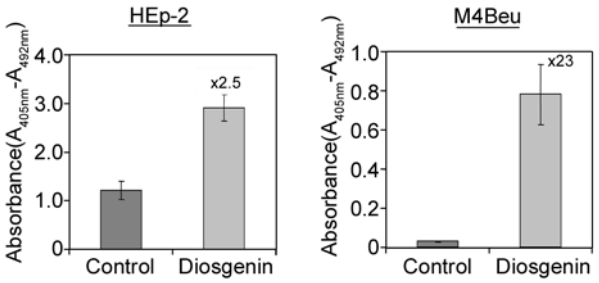

Fig 4. DNA fragmentation after diosgenin treatment. Apoptosis was quantified on floating and adherent cells using ELISA. Apoptotic ratio (top of diosgenin bar) was determined as sample absorbance/ control absorbance. Values are expressed as means ± SD (*p-value relative to control group, $p<0.05$).

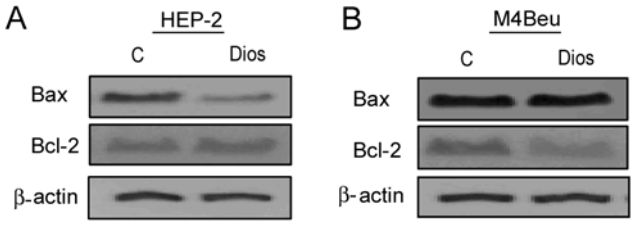

Fig 5. Bax and Bcl-2 analysis expression in HEp-2 and M4Beu cells. (A and B), Western blot analysis. HEp-2 and M4Beu cells were treated or not for 24 h with 40 μM diosgenin (Dios). Total protein was extracted from the cells and separated on 15% SDS-PAGE gel. Cellular expression of Bax, Bcl-2 and β-actin were estimated using mouse anti-human Bax, Bcl-2 and β-actin antibodies. Quantification of each band was performed by densitometry analysis software. One of three representative experiments is shown.

PARP cleavage was observed in M4Beu and HEp-2 cells after Western blot analysis: Fig 9 shows the native form (112 KD) and the 85 KD fragment of PARP. These results were confirmed by immunohistochemistry which indicates positive nuclear fluorescence for HEp-2 and M4Beu cells after diosgenin treatment compared with untreated controls.

DISCUSSION

It is of great importance to understand the mechanisms of apoptosis in cancer cells, as apoptosis is believed to be one of the major consequences of anticancer drug treatment against malignancies. Recently, we showed that three plant steroids had pro-apoptotic properties on osteosarcoma 1547 cells[16,17]. As diosgenin is the most effective in induction of apoptosis on 1547 cells[17], the aim of this study is to verify if its action was also similar on other cancer cell lines such as laryngocarcinoma HEp-2 cells and melanoma M4Beu cells. Our results showed that diosgenin strongly inhibited proliferation of HEp-2 and M4Beu cells and blocked the cell cycle as previously described in 1547 cells[16]. It is now established that the tumor suppressor p53 inhibits cell growth through activation of cell cycle arrest[3, 21] and apoptosis[22]. Regulation of p53 activity is through multiple mechanisms, one of which is phosphorylation[23]. Indeed, it was established

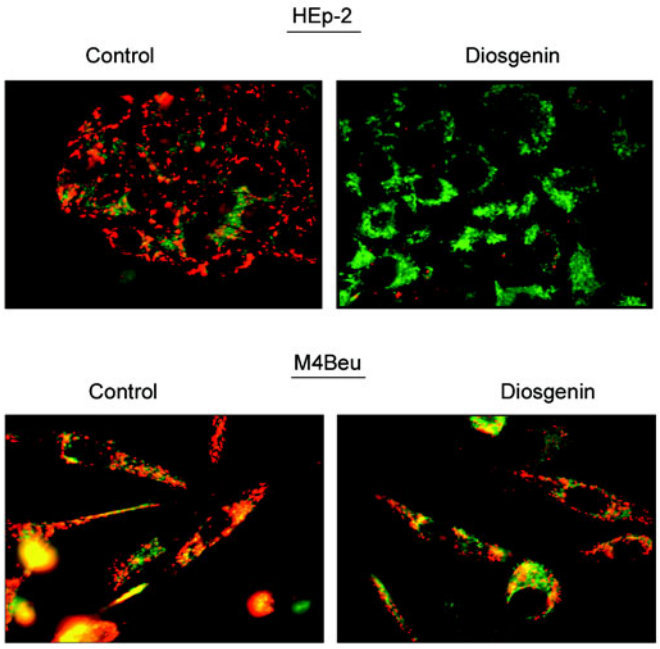

Fig 6. Mitochondrial membrane potential (Δψm) analysis after diosgenin treatment. Cells were cultured in 10% FCS medium during 3 d and treated or not with 40 µM diosgenin. After treatment, adherent cells were incubated with medium containing JC-1 (1µg/ml) for 30 min at 37°C. Red fluorescence represents mitochondria with intact membrane potential whereas green fluorescence represents de-energized mitochondria. Pictures were taken with a Nikon microscope ECLIPSE E800 (×400). One of three representative experiments is shown.

that phosphorylation of p53 protein may play a critical role in its stabilization, up-regulation, and functional activation[24]. We used antibody against p53 phosphoserine-392 to detect phosphorylation of p53 at serine 392. This site is involved in regulating the stabilization of p53 by enhancing tetramer formation. Then, this phosphorylation activates the DNA binding activity of p53. In our study, immunofluorescence revealed that treatment of HEp-2 and M4Beu cells with diosgenin markedly increased the cellular expression of activated p53 as previously described in 1547 cells[17]. Furthermore, diosgenin caused cell cycle arrest in S and G_2/M phases in HEp-2 and M4Beu cells respectively in contrast to 1547 cells which showed a cell cycle arrest in G_1[16]. It is known that p53 is involved in controlling entry into mitosis when cells enter G_2 with damaged DNA or when they are arrested in S phase due to depletion of substrates required for DNA synthesis[25]. Frey *et al*[26] showed that genistein, an isoflavone, caused a G_2/M block in cell cycle progression inducing p53.

Another mechanism by which diosgenin produced an anti-proliferative effect on cancer cells was the induction of apoptosis. To compare the effect of diosgenin on induction of apoptosis between 1547 cells[16] and two other cancer cell lines (HEp-2 and M4Beu), apoptosis was evaluated by ELISA performed on pooled cell fractions (floating and adherent). Moreover, the Bax/Bcl-2 ratio, which is a critical determinant of apoptosis[27, 28], was determined by Western blot analysis. In our conditions, the apoptotic ratio obtained by ELISA increased in HEp-2 and M4Beu cells as we described in 1547 cells[16]. Only Bax/Bcl-2 ratio was enhanced for M4Beu cells in contrast to HEp-2 cells. This result confirms that melanoma M4Beu cells with a high Bax/Bcl-2 ratio tend to have an increased apoptotic ratio after diosgenin treatment as observed in osteosarcoma 1547 cells[16]. A similar observation has also been reported in certain human melanoma cells, showing a significant correlation between CD95/Fas-mediated apoptosis and the Bax/Bcl-2 ratio[29].

Mitochondria have, apart from their function in respiration, an important role in the apoptotic-signalling pathway. Malfunctioning at any cellular level is eventually translated by the release of apoptogenic factors like cytochrome c and AIF from the mitochondrial intermembrane space resulting in the organized demise of the cell[30]. Mitochondria possess a latent mechanism called mitochondrial permeability transition (MPT) that, when activated, destroys this permeability barrier and disrupts normal mitochondrial function[31]. An important consequence of an activated MPT is that no transmembrane proton gradient can be maintained, thus abolishing the production of ATP. Moreover, it is well known that the modification of Δψm depends on the nature of stimulus and cell system

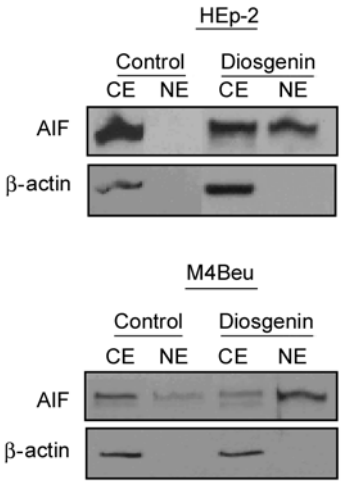

Fig 7. Effect of diosgenin on AIF subcellular redistribution. HEp-2 and M4Beu cells were cultured in 10% FCS medium and treated or not with 40 µM diosgenin for 6 h. Cytosolic and nuclear proteins were extracted as described in Materials and Methods and separated on 10% SDS-PAGE gels for AIF analysis. Immunoblot analyses were performed with anti-human AIF antibody for cytosolic extract (CE) and nuclear extract (NE). Quantification of each band was performed by densitometry analysis software. One of three representative experiments is shown.

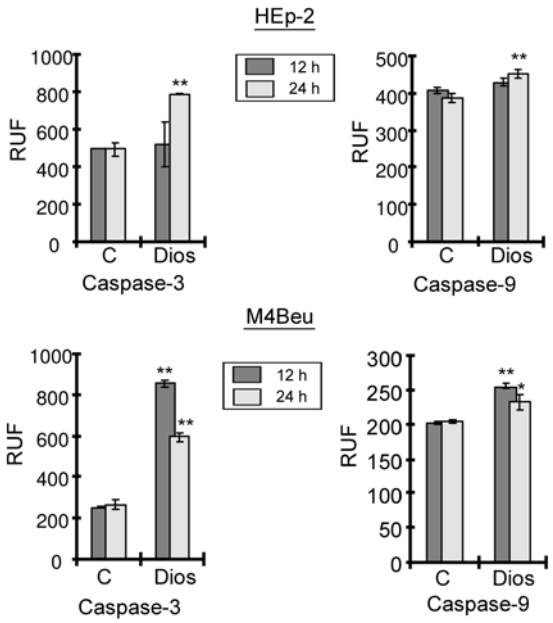

Fig 8. Caspase-3 and -9 activities in HEp-2 and M4Beu cells. After 72 h-adherence, cells were cultured in 10% FCS medium and treated or not (C, control) with 40 µM diosgenin (Dios) for 12 and 24 h. Caspase activities in cell lysates were measured with caspase-3 substrate (ac-DEVD-AMC) and caspase-9 substrate (ac-LEHD-AMC). The means ± SD (*p<0.05, **p<0.01) of three experiments are expressed as relative units of fluorescence (RUF).

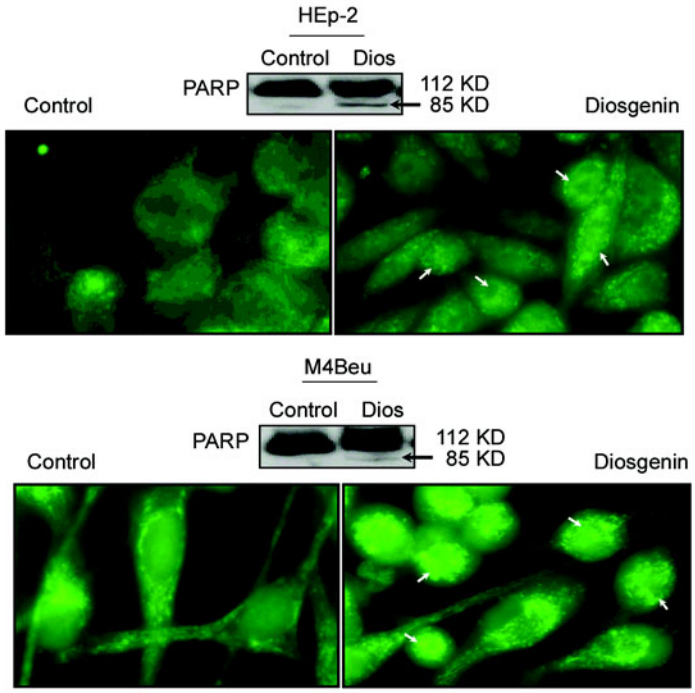

Fig 9. Analysis of PARP cleavage. For Western blot analysis, Hep-2 and M4Beu cells were cultured in 10% FCS medium and treated or not (control) with 40 µM diosgenin for 24 h. Total proteins were extracted and separated on 10% SDS-PAGE gel. Cellular expression of PARP was estimated using mouse anti-human PARP antibody. One of three representative experiments is shown. Arrows indicate the 85 kD fragment of PARP. For immunofluorescence detection of 85 kD fragment of PARP, HEp-2 and M4Beu cells were treated or not (control) with 40 µM diosgenin for 24 h. Immunofluorescence pictures were taken with a Nikon microscope ECLIPSE E800 (×500). White arrows indicate positive nuclear labelling.

and the collapse of $\Delta\psi m$ is an early step in the apoptotic cascade[32]. Recently, Diaz *et al* showed that dietary phytochemical chlorophyllin caused an attenuation of $\Delta\psi m$ without the release of cytochrome c and reported that AIF was released from mitochondria into the cytosol and translocated to the nucleus[33]. In this case, we showed the same phenomenon in HEp-2 cells: indeed, diosgenin caused a decrease of $\Delta\psi m$ and nuclear localization of AIF (Fig 6 and 7 respectively) without the release of cytochrome c (data not shown).

Other key proteins that modulate the apoptotic response are represented by a family of cysteine proteases called caspases[34, 35]. Caspase-3 is a key executioner of apoptosis, whose activation is mediated by the initiator caspases such as caspase-9[36]. We found that diosgenin induced caspase-3 activity over time in the two cancer cell lines studied. This activation seems to be the consequence of caspase-9 activity as a function of cancer cell type. Especially in M4Beu cells, caspases are activated sooner and more potently than in HEp-2 cells, suggesting that apoptotic events occured earlier. Recently, it was shown that rottlerin, an inhibitor of protein kinase C, increased the release of mitochondrial AIF to the cytosol, enhanced the activation of caspase-9 but did not increase cytochrome c in the cytosol[37]. Moreover, Susin *et al* described that AIF induced purified mitochondria to release the caspase-9[13]. In our study, diosgenin treatment in HEp-2 cells induced caspase-9 and -3 (Fig 8) with an early fall of $\Delta\psi m$ without cytochrome c release (data not shown) but with nuclear localization of AIF.

PARP is a nuclear enzyme involved in the repair of DNA damage[38]. Moreover, it is known that PARP is a substrate for caspases such as caspase-3 and is typically cleaved and inactivated during the apoptotic process[39]. In our work, we found a correlation between generation of a 85 kD degration product from 112 kD PARP and caspase-3 activity in HEp-2 and M4Beu cells. Following the apoptotic stimulus, numerous studies showed that caspase-3 activation caused cleavage of PARP[40, 41].

In summary, we demonstrated that diosgenin caused an inhibition of cell growth with cycle arrest and apoptosis induction by p53 activation in different human cancer cell lines (laryngocarcinoma and melanoma cells). Moreover, a large part of our study essentially focused on the mitochondrial pathway and we investigated that diosgenin's action was caspase-3 dependent, with a fall of $\Delta\psi m$ and nuclear localization of AIF. These new findings suggest that diosgenin-induced effects may have novel therapeutic applications for the treatment of different cancer types (laryngocarcinoma, melanoma) as previously described for osteosarcoma[16, 17].

ACKNOWLEDGEMENTS

We are grateful to Professor M. Cogné (Laboratoire d'Immunologie, Faculté de Médecine de Limoges, France) and Professor C. Delage (Laboratoire de Chimie Physique et Minérale, Faculté de Pharmacie de Limoges, France) for providing the cell lines. We would like to thank Dr J. Cook-Moreau for helpful discussions in the preparation of this manuscript. We also thank Dr. C. Jayat-Vignoles (Service Commun de Cytométrie, Université de Limoges) for valuable advice concerning flow cytometry analysis and A. Rametti and D. Léger for help in performing western blot experiments. The expenses of this work were defrayed in part by the Ministère de l'Education Nationale, de la Recherche et de la Technologie, the Conseil Régional du Limousin and by the Fond Social Européen.

Received, Dec 16, 2003
Revised, Jan 25, 2004
Accepted, Mar 5, 2004

REFERENCES

1 Vousden KH. Activation of the p53 tumor suppressor protein. Biochim Biophys Acta 2002; **1602**:47-59.
2 Moll UM and Zaika A. Nuclear and mitochondrial apoptotic pathways of p53. FEBS Lett 2001; **493**:65-9.
3 el-Deiry WS, Tokino T, Velculescu VE et al. WAF1, a potential mediator of p53 tumor suppression. Cell 1993; **75**:817-25.
4 Contente A, Dittmer A, Koch MC, Roth J, Dobbelstein M. A polymorphic microsatellite that mediates induction of PIG3 by p53. Nat Genet 2002; **30**:315-20.
5 Oren M. Decision making by p53: life, death and cancer. Cell Death Differ 2003; **10**:431-42.
6 Hengartner MO. The biochemistry of apoptosis. Nature 2000; **407**:770-6.
7 Zamzami N, Susin SA, Marchetti P et al. Mitochondrial control of nuclear apoptosis. J Exp Med 1996; **183**:1533-44.
8 Green DR, Reed JC. Mitochondria and apoptosis. Science 1998; **281**:1309-12.
9 Gottlieb RA. Mitochondria: execution central. FEBS Lett 2000; **482**:6-12.
10 Green D, Kroemer G. The central executioners of apoptosis: caspases or mitochondria? Trends Cell Biol 1998; **8**:267-71.
11 Cai J, Yang J, Jones DP. Mitochondrial control of apoptosis: the role of cytochrome c. Biochim Biophys Acta 1998; **1366**:139-49.
12 Daugas E, Nochy D, Ravagnan L, et al. Apoptosis-inducing factor (AIF): a ubiquitous mitochondrial oxidoreductase involved in apoptosis. FEBS Lett 2000; **476**:118-23.
13 Susin SA, Lorenzo HK, Zamzami N, et al. Molecular characterization of mitochondrial apoptosis-inducing factor. Nature 1999; **397**:441-46.
14 Daugas E, Susin SA, Zamzami N, et al. Mitochondrio-nuclear translocation of AIF in apoptosis and necrosis. FASEB J 2000; **14**:729-39.
15 Gordon J, Wu CH, Rastegar M, Safa AR. Beta2-microglobulin induces caspase-dependent apoptosis in the CCRF-HSB-2 human leukemia cell line independently of the caspase-3, -8 and -9

pathways but through increased reactive oxygen species. Int J Cancer 2003; **103**:316-27.
16 Moalic S, Liagre B, Corbiere C, et al. A plant steroid, diosgenin, induces apoptosis, cell cycle arrest and COX activity in osteosarcoma cells. FEBS Lett 2001; **506**:225-30.
17 Corbiere C, Liagre B, Bianchi A, et al. Different contribution of apoptosis to the antiproliferative effects of diosgenin and other plant steroids, hecogenin and tigogenin, on human 1547 osteosarcoma cells. Int J Oncol 2003; **22**:899-905.
18 Moalic S, Liagre B, Labrousse F, Beneytout JL. Enhanced apoptosis in retrovirally transfected osteosarcoma cells after exposure to sodium butyrate. Int J Oncol 2000; **16**:695-700.
19 Smiley ST, Reers M, Mottola-Hartshorn C, et al. Intracellular heterogeneity in mitochondrial membrane potentials revealed by a J-aggregate-forming lipophilic cation JC-1. Proc Natl Acad Sci USA 1991; **88**:3671-5.
20 Duval R, Bellet V, Delebassee S, Bosgiraud C. Implication of caspases during maedi-visna virus-induced apoptosis. J Gen Virol 2002; **83**:3153-61.
21 Kim TK. *In vitro* transcriptional activation of p21 promoter by p53. Biochem Biophys Res Commun 1997; **234**:300-2.
22 Blagosklonny MV. P53: an ubiquitous target of anticancer drugs. Int J Cancer 2002; **98**:161-6.
23 Meek DW. Multisite phosphorylation and the integration of stress signals at p53. Cell Signal 1998; **10**:159-66.
24 Shieh SY, Ikeda M, Taya Y, Prives C. DNA damage-induced phosphorylation of p53 alleviates inhibition by MDM2. Cell 1997; **91**:325-34.
25 Taylor WR, Stark GR. Regulation of the G2/M transition by p53. Oncogene 2001; **20**:1803-15.
26 Frey RS, Li J, Singletary KW. Effects of genistein on cell proliferation and cell cycle arrest in nonneoplastic human mammary epithelial cells: involvement of Cdc2, p21(waf/cip1), p27(kip1), and Cdc25C expression. Biochem Pharmacol 2001; **61**:979-89.
27 Oltvai ZN, Milliman CL, Korsmeyer SJ. Bcl-2 heterodimerizes in vivo with a conserved homolog, Bax, that accelerates programmed cell death. Cell 1993; **74**:609-19.
28 Reed JC, Jurgensmeier JM, Matsuyama S. Bcl-2 family proteins and mitochondria. Biochim Biophys Acta 1998; **1366**:127-37.
29 Raisova M, Hossini AM, Eberle J. The Bax/Bcl-2 ratio determines the susceptibility of human melanoma cells to CD95/Fas-mediated apoptosis. J Invest Dermatol 2001; **117**:333-40.
30 van Gurp M, Festjens N, van Loo G, Saelens X, Vandenabeele P. Mitochondrial intermembrane proteins in cell death. Biochem Biophys Res Commun 2003; **304**:487-97.
31 Kowaltowski AJ, Castilho RF, Vercesi AE. Mitochondrial permeability transition and oxidative stress. FEBS Lett 2001; **495**: 12-15.
32 Liu X, Kim CN, Yang J, Jemmerson R, Wang X. Induction of apoptotic program in cell-free extracts: requirement for dATP and cytochrome c. Cell 1996; **86**:147-57.
33 Diaz GD, Li Q, Dashwood RH. Caspase-8 and apoptosis-inducing factor mediate a cytochrome c-independent pathway of apoptosis in human colon cancer cells induced by the dietary phytochemical chlorophyllin. Cancer Res 2003; **63**:1254-61.
34 Alnemri ES, Livingston DJ, Nicholson DW et al. Human ICE/CED-3 protease nomenclature. Cell 1996; **87**:171.
35 Stennicke HR, Salvesen GS. Caspases - controlling intracellular signals by protease zymogen activation. Biochim Biophys Acta 2000; **1477**:299-306.
36 Salvesen GS, Dixit VM. Caspases: intracellular signaling by proteolysis. Cell 1997; **91**:443-6.
37 Basu A, Johnson DE, Woolard MD. Potentiation of tumor necrosis factor-alpha-induced cell death by rottlerin through a cytochrome-c-independent pathway. Exp Cell Res 2002; **278**: 209-14.
38 D'Amours D, Desnoyers S, D'Silva I, Poirier GG. Poly(ADP-ribosyl)ation reactions in the regulation of nuclear functions. Biochem J 1999; **342**:249-68.
39 Nicholson DW. Caspase structure, proteolytic substrates, and function during apoptotic cell death. Cell Death Differ 1999; **6**: 1028-42.
40 Jiang XH, Wong BC, Yuen ST et al. Arsenic trioxide induces apoptosis in human gastric cancer cells through up-regulation of p53 and activation of caspase-3. Int J Cancer 2001; **91**:173-9.
41 Yang WL, Addona T, Nair DG, Qi L, Ravikumar TS. Apoptosis induced by cryo-injury in human colorectal cancer cells is associated with mitochondrial dysfunction. Int J Cancer 2003; **103**: 360-9.